ACS APPLIED MATERIALS & INTERFACES

RESEARCH ARTICLE

www.acsami.org

Toward Homogeneous Nanostructured Polyaniline/Resin Blends

Shadi Jafarzadeh,*[,†] Esben Thormann,[†] Ted Rönnevall,[‡] Arindam Adhikari,[§] Per-Erik Sundell,[⊥] Jinshan Pan,[†] and Per M. Claesson[†,#]

[†]Division of Surface and Corrosion Science, School of Chemical Science and Engineering, Royal Institute of Technology (KTH), Drottning Kristinas väg 51, SE-100 44 Stockholm, Sweden

[‡]TEAMATOR AB, SE-250 23 Helsingborg, Sweden

[§]Functional Materials Division, Central Electrochemical Research Institute (CECRI/CSIR), Karaikudi, 630006, India

[⊥]SSAB EMEA, SE-781 84 Borlänge, Sweden

[#]Institute for Surface Chemistry (YKI), P.O. Box 5607, SE-114 86 Stockholm, Sweden

ABSTRACT: The high interest in applications of conducting polymers, especially polyaniline (PANI), makes it important to overcome limitations for effective usage due to poor processability and solubility. One promising approach is to make blends of PANI in polymeric resins. However, in this approach other problems related to the difficulty of achieving a homogeneous PANI dispersion arise. The present article is focused on this general problem, and we discuss how the synthesis method, choice of dopant and solvent as well as interfacial energies influence the dispersibility. For this purpose, different synthesis methods and dopants have been employed to prepare nanostructures of polyaniline. Dynamic light scattering analysis of dispersions of the synthesized particles in several solvents was employed in order to understand how the choice of solvent affects PANI aggregation. Further information on this subject was achieved by scanning electron microscopy studies of PANI powders dried from various solutions. On the basis of these results, acetone was found to be a suitable dispersion medium for PANI. The polymer matrix used to make the blends in this work is a UV-curing solvent-free resin. Therefore, there is no low molecular weight liquid in the system to facilitate the mixing process and promote formation of homogeneous dispersions. Thus, a good compatibility of the components becomes crucial. For this reason, surface tension and contact angle measurements were utilized for characterizing the surface energy of the PANI particles and the polyester acrylate (PEA) resin, and also for calculating the interfacial energy between these two components that revealed good compatibility within the PANI/PEA blend. A novel technique, based on centrifugal sedimentation analysis, was employed in order to determine the PANI particle size in PEA resin, and high dispersion stability of the PANI/PEA blends was suggested by evaluation of the sedimentation data.

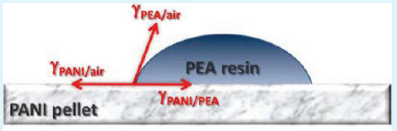

Interfacial energies in PANI/resin blends

KEYWORDS: conducting polymer, polyaniline, synthesis methods, particle size, interfacial energy, dispersion stability, LUMiSizer dispersion analyzer

1. INTRODUCTION

During the last decades, intrinsically conducting polymers (ICPs) have captured high attention in different applications because of their interesting and tunable properties.[1] Polyaniline (PANI) is one of the mostly used conducting polymers[2] because of low cost and ease of synthesis, high environmental and chemical stability, wide controllable range of electrical conductivity by simple doping/dedoping, and reversible redox property. A comprehensive list of possible applications of PANI related to each of its special properties is provided in the review article by Bhadra et al.[2] In many applications, especially in coatings technology, PANI is blended into a host polymer matrix and used as a conductive composite. In this way one may achieve the desired properties for each application by varying the polymer matrix, provided there is good compatibility between the composite components. However, problems like weak processability and poor solubility in most of the available solvents limit the effective usage of PANI, especially in the doped state where the high charge density results in a very high solubility parameter.[3] Different methods such as melt mixing, mill mixing, solution/dispersion mixing, in situ polymerization, electrochemical polymerization, and thermal reflux for preparation of polymer-based conducting composites from polyaniline have been discussed in the literature,[2] among which the solution/dispersion method is of interest for the present work.

Dispersion homogeneity is an important factor for making composites with uniform properties. It has been shown that nanostructures of PANI are preferred for achieving good dispersibility and processability,[4] improved interactions with the environment and faster response in sensor applications,[5] and a low percolation threshold[6−8] that is favorable for making transparent conducting blends and for retaining the mechanical properties of the host insulating polymer.

Generally, the PANI particle size has been found to be affected by different factors like reactant concentrations, reaction time, temperature, and synthesis method.[9] There have been several

Received: February 19, 2011
Accepted: April 11, 2011
Published: April 11, 2011

attempts reported in the literature using steric stabilizers,[8,10,11] surfactants,[12] various types of templates[13−17] or self-assembly[9,18] to produce submicrometer and nanosized PANI fibers and particles. However, simple ways for preparation of PANI nanostructures is still a scientific challenge. The most common way to synthesize polyaniline is chemical oxidative polymerization of aniline. Due to the exothermic process, synthesis has conventionally been done by adding the oxidant dropwise to the monomer.[19] However, it has been found that the polymer nanostructures produced in early stages form agglomerates due to secondary growth of irregularly shaped particles during polymerization.[4]

The main focus in the present work is on the methods suggested by Huang et al.[5] to produce small-diameter PANI, with no need for any external template or surfactant. One of these methods, the interfacial polymerization method, is based on keeping the monomer and oxidant in two different phases during polymerization in order to minimize contacts of reaction sites and thus counteract aggregate formation. The drawback is that only small amount of polymer is produced. The other method suggested by Huang et al. is based on rapid mixing, where small particles are achieved, presumable by suppressing the overgrowth due to the rapid consumption of reactant molecules and reduction in reaction time during polymerization.

Achieving homogeneous composite dispersions of PANI in insulating polymers requires not only proper control of the PANI morphology and size, but also a comprehensive knowledge of the polymer matrix and other components characteristics. A "nonequilibrium" or "dynamic" model of the dispersion is suggested in the literature[20] and it explains how spherical dispersed powders can percolate in a polymer blend by forming network-like flocculates as the liquid layers adsorbed on the filler particles come into contact above a critical volume concentration. Thus, the polymer matrix should be chosen such that formation of large PANI aggregates is counteracted, meaning that the interfacial forces within the composite and accordingly the PANI critical concentration have to be controlled.[3] The system can also be improved by using proper additives, like plastisizers.[21] Solution processing of emeraldine base in N-methylpyrrolidone[22] or emeraldine salt in concentrated sulfuric and other strong acids[23] has also been reported as a way to fabricate PANI dispersions in an insulating polymer matrix that is soluble in the same solvent. Counterion-induced processability of PANI, i.e. using protonic acid dopants with counterion species compatible with specific organic liquids, has been another approach.[24] However, the suggested solvents are mostly toxic, dispersions are stable with only very low concentrations of PANI, and these approaches limit the usage of most commercial polymers, which are cosoluble in other organic solvents, and high solid, solvent-free resins.

The emphasis of the present work is on the dispersion behavior of PANI in solvents and a UV-curing polymer resin to facilitate homogeneous PANI/resin blends, which can potentially be used as conductive composite coatings. PANI was synthesized by three different methods in the presence of methane sulfonic acid (MeSA) or phosphoric acid (PA) dopants. The conductivity, structural characteristics, particle size and morphology of the synthesized PANIs were investigated by a multianalytical approach. The compatibility of the composite components was evaluated by contact angle and surface tension measurements that allowed calculations of the interfacial energy between conducting PANI and insulating resin. Centrifugal sedimentation analysis of the PANI/resin dispersion was carried out to investigate the stability of the dispersion and particle size distribution directly in the resin matrix. It should be noted that the polymer matrix studied in this work is a high solid resin which, compared to solvent-based systems, makes it more difficult to prepare the PANI/resin dispersions. Thus, the choice of resin, its compatibility with the system components, and the particle preparation before blending into the polymer matrix is of high importance.

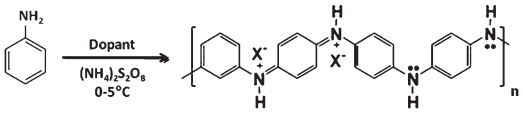

Figure 1. Reaction scheme for synthesis of polyaniline. Right side shows the schematic structure of polyaniline in emeraldine salt state, and X^- is the counterion.

2. EXPERIMENTAL SECTION

2.1. Materials. The chemicals used for synthesis of the conducting polymer were aniline (Aldrich grade, 99%), methane sulfonic acid (MeSA) (Aldrich grade, purity ≥99%), phosphoric acid (Sigma-Aldrich, 99%), ammonium peroxodisulfate (APS) (Merck grade, 99%), ethanol (Merck grade 99.9%), and xylene (Fluka, purity ≥99%). Other solvents used in the characterization tests were acetone (Merck grade, purity ≥99.8%), n-methyl pyrrolidion (NMP) (VWR, purity >99%) and chloroform (Aldrich grade, for analysis).

The resin used was UV-curing polyester acrylate (PEA), a laboratory formulation provided by Cytec Surface Specialties to be used as primer organic coating. The formulation is based on a chlorinated polyester diluted with hexanediol diacrylate (to a mass ratio of 3:2), with a photo initiator to facilitate radical-type polymerization while exposed to UV light and phosphorus-containing acidic methacrylate as adhesion promoter.

2.2. Synthesis of Polyaniline. Three synthesis methods were employed to prepare PANI. These methods will be referred to as "conventional", "rapid mixing" and "interfacial polymerization". In all cases, PANI was synthesized by chemical oxidative polymerization of aniline with ammonium peroxodisulfate as oxidant, in presence of methane sulfonic acid or phosphoric acid aqueous solution as dopant. The process is schematically shown in Figure 1.

The dopant anion for PANI-MeSA is $CH_3SO_3^-$.[25] For PANI-PA dihydrogen phosphate ($H_2PO_4^-$), hydrogen phosphate (HPO_4^{2-}) and eventually phosphate (PO_4^{3-}) anions are present as a result of different dissociation levels of phosphoric acid depending on the acidity of the medium.[26]

2.2.1. Conventional Synthesis. In the conventional synthesis method,[19] the oxidant solution (0.11 molar ammonium peroxodisulfate in ultrapure water) is added dropwise (by a rate of 0.1 mLs^{-1}) to a solution of 0.1 molar aniline and 0.1 molar dopant (methane sulfonic acid or phosphoric acid) in ultrapure (Milli Q) water. The reaction is carried out at a temperature of 0−5 °C with ice around the reaction vessel for 12 h under stirring (1500 rpm). The controlled low temperature is chosen to prevent high increase in temperature due to the exothermic reactions, and also to limit the diffusion mobility of particles and, as a consequence, slow down aggregation. The polymer obtained was in the conducting state (green color of doped PANI; emeraldine salt state). The reaction product was separated from the solution by filtration and washed with ultrapure water (Milli Q) several times, followed by rinsing with ethanol to remove residual monomers and other impurities. The powders were then dried at room temperature in a desiccator (with silica gel desiccant).

2.2.2. Rapid Mixing. In the rapid mixing method,[4] oxidant is added to the aniline/dopant solution all at once, with a monomer:dopant:oxidant molar ratios of 1:2:1.1. Compared to the conventional method we used

half the concentration (in order to minimize the risk due to the exothermic reaction), and the shorter reaction time was the reason for using double amount of dopant. The temperature of the reaction vessel was kept at 0−5 °C with ice around and the polymer appeared first in nonconducting state (blue color), which turned into the conducting state by further mixing (dark green color in less than one hour). After 12 h of stirring (1500 rpm), the polymer was filtered and collected following the same procedure as for the conventionally synthesized polymer.

2.2.3. Interfacial Polymerization. Interfacial polymerization of aniline[4] is done in a separating funnel where reactions take place at the phase boundary of an immiscible aqueous/organic biphasic system at room temperature. No cooling is needed as the reactions proceed gradually (limited by the number of reactants at the interface) and there is no stirring of the system. The organic medium was xylene, and aniline monomer was added to this phase to a concentration of 0.1 molar. The aqueous phase contained 0.11 molar ammonium peroxodisulfate and 1.5 molar dopant (methane sulfonic acid or phosphoric acid) in ultrapure (Milli Q) water. Generally, in most aqueous and organic systems, PANI is formed in the aqueous phase since protonated PANI in the emeraldine salt form is hydrophilic in nature.[26] Here, the blue color of PANI started to appear at the interface a few minutes after pouring the two solutions into the separating funnel, and by further reaction with the dopant the green (doped) polymer moved into the aqueous medium. The polymer was collected after 12 h.

2.3. Characterization of the Synthesized Polyaniline.

2.3.1. Impedance Spectroscopy for Conductivity Measurement. A pressed pellet of PANI with 0.15 cm thickness, l, and 1.28 cm diameter, d, was placed tightly between two gold plate electrodes connected to a Solartron 1296 electrochemical interface coupled to a Solartron 1260 frequency response analyzer, and the impedance spectrum was measured with an AC amplitude of 10 mV and frequency range from 1 MHz to 0.1 Hz. The measurements were repeated after different time intervals until a stable condition was reached. The resistance at low frequency, R, was collected and analyzed by the SMaRT software, from Solartron Analytical. The conductivity, σ, was then calculated as $\sigma = (4l)/(\pi d^2 R)$.

2.3.2. Spectroscopic and Diffraction Techniques. The molecular structure of the PANIs was characterized by infrared spectroscopy (attenuated total reflectance, ATR), UV−visible absorption spectroscopy, and X-ray diffraction (XRD). The ATR-IR spectrum of the polymer in powder form was obtained by using a PerkinElmer IR spectrometer controlled by Spectrum One (with a frequency range of 1800−600 cm^{-1}). The UV−vis spectrum of PANI solution in chloroform was recorded by a LAMBDA 650 spectrophotometer (PerkinElmer Inc., USA) in the range of 300−900 nm. A X' Pert Pro MPD X-ray diffractometer (PAN analytical, The Netherlands) equipped with a Cu Kα X-ray source was used to obtain the XRD graphs. The wavelength of the beam and the scan range (2θ) were 1.54178 Å and 5−50°, respectively.

2.3.3. Dynamic Light Scattering (DLS). Samples of PANI-MeSA and PANI-PA were dispersed in several solvents with different dielectric constants (water (ε_r = 80), n-methyl pyrrolidion (NMP) (ε_r = 32), acetone (ε_r = 21) and chloroform (ε_r = 4.8)) to a concentration of 0.03 g L^{-1} and sonicated for about 4 h by a SONICS Vibra cell, Model VC750, with a max power of 750W. The (unfiltered) samples were characterized by dynamic light scattering (DLS) conducted with a Brookhaven Instruments (USA) device, which consists of a BI-200SM goinometer and a BI-9000AT digital autocorrelator. The light source was a water-cooled argon-ion laser, Lexel 95 model 2, with a maximum power of 2 W and a wavelength of 514.5 nm. The liquid around the sample holder was decahydronaphtalene. The diffusion coefficients were determined from the decay time of the autocorrelation function measured at a scattering angle of 90°. The Inverse Laplace Transformation analysis was performed by the Contin (Non-negatively constrained least-squares; regularized) method.[27] The effective hydrodynamic radius, R, of the objects in the fluid was calculated from the measured diffusion constant distribution, D, using the Stokes−Einstein equation for spherical particles: $R = (K_B T)/(6\pi\eta D)$ where k_B is the Boltzmann constant, T is the temperature and η is the viscosity. For nonspherical particles, the equivalent hydrodynamic radius is presented, which is the hydrodynamic radius of a hard sphere with the same diffusion constant as the scattering object. More information on the theory behind light scattering measurements can be found in the literature (e.g., ref 28).

Table 1. Surface Energy Properties (mJ m^{-2}) of Liquids Used for Contact Angle Measurements[29]

liquid	γ_L	γ^{LW}	γ^{AB}	γ^+	γ^-
diiodomethane	50.8	50.8	≈0	≈0	0
water	72.8	21.8	51.0	25.5	25.5
ethylene glycol	48.0	29.0	19.0	1.92	47.0

2.3.4. Scanning Electron Microscopy (SEM). The morphology of the polymer powders was examined by high resolution scanning electron microscopy (SEM), using a FEI COMPANY (Claymount, The Netherlands) instrument. The samples were prepared by depositing one drop of a sonicated PANI containing solution on a glass plate and allowing it to dry in a desiccator (with silica gel desiccant) for 24 h, followed by gold sputtering with a current of 40 mA for 40 s.

2.4. Contact Angle and Surface Tension Measurements.

The compatibility between conducting polymer and resin was examined by comparing the materials interfacial tension, which provides a quantitative expression for the free energy of the interparticle interaction.[29] This was achieved by contact angle measurements on smooth films of the resin and PANIs. Uniform films of PEA resin were applied on polished carbon steel using a spin coater (Headway Research Inc.). The films were then UV-cured by employing a Fusion UV curing instrument, Model MC6R (Fusion Systems Corporation, USA) with P300 M power supply and UV lamp irradiance of 120 ± 5 W cm^{-2} in the UV-A region. PANI powders were pressed into pellets using the same procedure as for the samples prepared for conductivity measurements. Contact angles were assessed with an OCA20 instrument (DataPhysics, Germany), and measurements were done by the sessile drop method. The liquid droplet is illuminated while being dispensed (with a volume of 4 μL) on the surface, and the variation in drop shape is captured by a high resolution CCD camera. By examining the recorded series of images afterward, the first point of droplet relaxation equilibrium is found and used for the contact angle determination, done by the SCA20 software using the Ellipse fitting method.

Contact angle liquids were chosen according to the requirements to solve eq 1, which arises from the Good−Girifalco−Fowkes combining rule for interfacial Lifshitz-van der Waals interactions with the Young−Dupré equation considering acid−base interactions.[30]

$$(1+\cos\theta)\gamma_L = 2\left(\sqrt{\gamma_S^{LW}\gamma_L^{LW}} + \sqrt{\gamma_S^{+}\gamma_L^{-}} + \sqrt{\gamma_S^{-}\gamma_L^{+}}\right) \quad (1)$$

Where θ is the contact angle between a droplet of a known liquid L and a solid S, γ is the surface energy, γ^{LW} is the Lifshitz-van der Waals (apolar) component of the surface energy, γ^+ is the electron-acceptor surface energy parameter and γ^- is the electron-donor surface energy parameter of the material. γ^+ and γ^- are nonadditive parameters of the Lewis acid−base (polar) component of the surface energy; $\gamma^{AB} = 2(\gamma^+\gamma^-)^{1/2}$.

It is important that $\gamma_L > \gamma_S$ to obtain a finite contact angle and thus liquids with high surface energy (diiodomethane, water, and ethylene glycol) were chosen for the measurements. The surface energy properties of these liquids can be found in the literature,[29] and are reproduced in Table 1.

The surface energy of liquid PEA in air was determined by the Pendant drop method.[31,32]

Table 2. Conductivity of the Doped PANIs Synthesized by Different Methods[a]

	conventional synthesis		rapid mixing		interfacial polymerization	
	PANI-PA	PANI-MeSA	PANI-PA	PANI-MeSA	PANI-PA	PANI-MeSA
σ (S cm^{-1})	7.3×10^{-2}	2.4×10^{-1}	9.7×10^{-2}	6.0×10^{-1}	1.1×10^{-1}	8.1×10^{-1}

[a] The conductivity was calculated from the data obtained by impedance spectroscopy on pressed pellets of PANI.

The wettability of liquid PEA on PANI pellet surfaces was investigated by visually following the variations in the PEA drop shape.

2.5. Dispersion Stability and PANI Particle Size Distribution in Liquid PEA Resin. Blends were made by mixing 0.05, 0.5, 1.5, and 4 wt.% of PANI powders with liquid PEA resin. The PANI powders were prepared by evaporation from PANI/acetone solution under sonication, and were then added to the resin in small portions under mixing, followed by 24 h stirring using a magnetic stirrer (1200 rpm).

Centrifugal Sedimentation. Sedimentation of PANI in liquid PEA resin under centrifugal forces was followed using a microprocessor controlled analytical centrifuge; LUMiSizer dispersion analyzer, model 611 (L.U.M., GmbH Berlin), and the results were analyzed with the SEPView 5.1 software. The intensity of the transmitted NIR-LED (880 nm) light over the full sample length was detected by a CCD-Line (2048 elements) sensor, and the extinction profiles were recorded as a function of time and radial position during centrifugation. Details of the technique are described in ref 33. The samples were filled into cuvettes made of polyamide with an optical path length of 2.2 mm, and the test was performed at 25 °C with a rotation speed of 4000 rpm. The extinction profiles were recorded with 300s time intervals.

The dispersion stability was evaluated from the integral of the transmission profiles between the bottom and the fluid level.[34,35] The particle size distribution was evaluated from the light transmission variation as a function of the radial sample position over a defined time interval, using the "constant time" method.[36] Briefly, the measured transmission values, T, are transformed into extinction values, E, using the equation $E = -\ln[T/T_0]$, where T_0 is the transmission of the sample cell filled with the dispersion medium only. By invoking Stokes law, the particle size (equivalent sphere size) is calculated according to eq 2.

$$x = \sqrt{\frac{18\eta_F}{(\rho_P - \rho_F)\omega^2 t_m} \ln\left(\frac{r_m}{r_0}\right)} \quad (2)$$

Where x is the PANI particle size, η_F is the PEA fluid viscosity, ρ_P and ρ_F correspond to the densities of PANI powder and PEA fluid, r_0 is the starting position of the particles, r_m and t_m are the measurement position and time, respectively and ω is the angular frequency. With the constant time method, the cumulative volume or number weighted particle size distribution is then calculated directly from the extinction profiles using eq 3.

$$Q_3(x) = \frac{\int_{E_{min}}^{E(r)} \frac{r^2}{A_v(x)} dE(r)}{\int_{E_{min}}^{E_{max}} \frac{r^2}{A_v(x)} dE(r)} \quad (3)$$

Where A_v is the volumetric cross section, and this quantity is calculated by the instrument software using Mie theory.[36] These data are, theoretically, comparable with results from other laser diffraction and centrifugal techniques.[37]

The viscosity of the PEA fluid as well as the density and refractive index of both PEA and PANI powder are needed for the particle size calculations. For the liquid PEA resin, the density is found to be 1.372 g cm^{-3}, the viscosity at 25 °C is 1750 mPa s, as measured by a Bohlin Gemini Rheometer 150, and the refractive index is 1.525, as measured by an Abbé Refractometer, model A (Carl Zeiss, Germany). The density of the PANI-PA powder was measured by examining the volume change in water by adding grinded powders of known mass, and found to be 1.769 g cm^{-3}. The refractive index of PANI-PA was determined by a phase modulated ellipsometer (Beaglehole Instruments) using the smooth surface of a pressed PANI pellet, and the real and imaginary parts of the refractive index of PANI-PA were calculated to be 1.48 and 0.208, respectively.

3. RESULTS AND DISCUSSION

3.1. Characterization of Doped Polyaniline. *3.1.1. Conductivity.* The conductivity of PANI-MeSA and PANI-PA polymers, synthesized by the three described methods, was found to be in the order of 10^{-2} to 10^{-1} S cm^{-1} (see Table 2), which is in the range of good semiconductors and consistent with values reported in the literature.[26]

3.1.2. Molecular Structure Characterization. The spectroscopic characterization of the PANI samples confirmed the characteristic peaks of polyaniline, and showed them to be in the emeraldine (salt) state (schematically shown in Figure 1). Examples of the results are shown in Figure 2 for PANI-PA prepared by conventional synthesis, and similar results were obtained for the other samples, in accordance with the previously published data for PANI-MeSA.[25]

In the ATR-IR spectrum (Figure 2a), the presence of two bands in the vicinity of 1570 and 1485 cm^{-1} are assigned to the nonsymmetric aromatic ring stretching modes, where the higher frequency vibration at 1570 cm^{-1} is due to the quinoid rings arising from both C═N and C═C stretching of the quinoid diimine unit (N=Q=N),[25,38,39] whereas the one at 1485 cm^{-1} is due to the C−C aromatic ring stretching of the benzenoid diamine unit (N−B−N).[25,39,40] The peaks around 1300 and 1250 cm^{-1} correspond to the C−N stretching vibration of secondary aromatic amine,[38,39] and the peak at 1125 cm^{-1} is assigned to aromatic C−H in-plane bending.[38,40] The broad band around 1050 cm^{-1} is a fingerprint arising from the combination of dopant anions; $H_2PO_4^-$ and HPO_4^{2-} moieties[41] and/or tetrahedral PO_4^{3-} vibration,[26] which confirms the presence of dopant anions on the chain. The peak close to 800 cm^{-1} is due to out-of-plane deformation of C−H of 1,4-disubstituted rings.[25,38,40]

In the UV−vis absorption spectrum (Figure 2b); the characteristic peak at around 330 nm can be assigned to $\pi-\pi^*$ transition of the benzenoid rings[38,39] (the red-shift of the peak in the spectrum shown in Figure 2b could be due to the molecular weight dependence of this peak position[42]), whereas the peaks at around 450 and 820 nm can be attributed to the polaron$-\pi^*$ and $\pi-$polaron transitions, respectively.[9,39] The peak at around 800 nm is known as a sign of protonation of the emeraldine form of PANI.[42]

The XRD pattern of PANI-PA (Figure 2c) shows an intense peak at a 2θ value of about 25°, which is reported as the

Table 3. Particle Size Range (nm) Detected by DLS for PANI-PA and PANI-MeSA Dispersed in Acetone, Chloroform, and Water

	conventional synthesis		rapid mixing		interfacial polymerization	
solvent	PANI-PA	PANI-MeSA	PANI-PA	PANI-MeSA	PANI-PA	PANI-MeSA
acetone	90−160	90−115	55−85	75−115	50−110	40−95
chloroform	320−860	345−1150	185−320	200−350	130−400	100−300
water	340−1250[a]	610−900	320−410	360−440	120−350	180−560

[a] Also some particles of >3 μm.

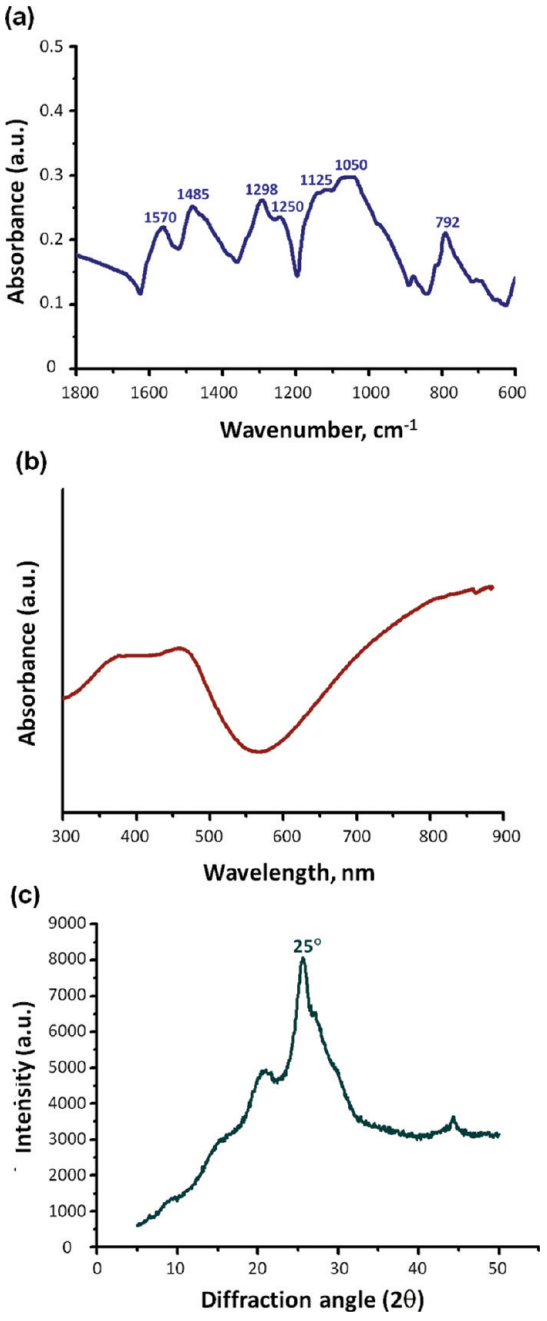

Figure 2. (a) ATR-IR, (b) UV−vis absorption, and (c) XRD spectra for PANI-PA.

characteristic peak for polyaniline in the literature.[25,38] The interatomic spacing (d) corresponding to the X-ray intensity peak at $2\theta \approx 25°$ is calculated to be 3.6 Å using Bragg's law. The d-spacing and interchain separation affect the polymer conductivity as a decrease in d-spacing results in increased probability of interchain hopping of charge carriers and hence higher conductivity.[2] The broad peak centered around $2\theta \approx 25°$ demonstrates the predominant amorphous structure of polyaniline. However, the presence of some sharp peaks indicates some crystallinity of the sample. Crystallinity also affects the intramolecular mobility of charged species along the chain and the intermolecular hopping of charge carriers, thus higher crystallinity and more organized structure lead to increased conductivity.[2]

3.1.3. PANI Particle Size Distribution in Solvents. DLS was performed on dispersions of PANI particles in several solvents after 4 h ultrasonication. No data could be achieved from NMP solutions due to the small scattering contrast between NMP and PANI (refractive index is 1.47 for NMP and 1.48 for PANI). The PANI particle size in acetone, chloroform and water dispersions are shown in Table 3.

Independent of synthesis method and dopant type (MeSA or PA), the particle size was found to mainly depend on the solvent in the following order: $PANI_{in\ acetone} < PANI_{in\ chloroform} < PANI_{in\ water}$. The particle size range in chloroform and water was considerably broader for conventionally synthesized polymers as compared to other synthesis methods. Since PANI powders from the same synthesis batch were used in all solvents, we conclude that the difference observed is due to different levels of aggregation in the corresponding solvents, and that acetone is the best dispersion medium of the solvents tested. Thus, for the rest of the discussion, we focus on DLS results obtained with acetone as solvent.

The particle size (effective hydrodynamic diameter) distributions, based on the number of particles with a given size, of PANI-PA and PANI-MeSA synthesized by the three discussed methods and dispersed in acetone are shown in Figure 3. The results indicate rather narrow size distribution profiles for PANI particles in acetone, with interfacial polymerization providing the smallest particles. More than 90% of the particles are less than 100 nm when synthesized by interfacial polymerization or rapid mixing, whereas for the polymers made by the conventional synthesis method, slightly larger particles were detected.

It is concluded that the synthesis method and solution media control the particle size distribution, while altering between phosphoric and sulfonic acid based dopants does not have any significant effect on the particle size. Since rapid mixing synthesis provides significantly more material than interfacial polymerization, and only slightly larger particles, PANI prepared by the rapid mixing process was chosen for further studies.

3.1.4. Morphology. SEM images of PANI-PA synthesized by rapid mixing after drying from solutions of different solvents are shown in Figure 4.

The drying process clearly causes aggregation, and the morphology of the aggregates formed during drying depends on the

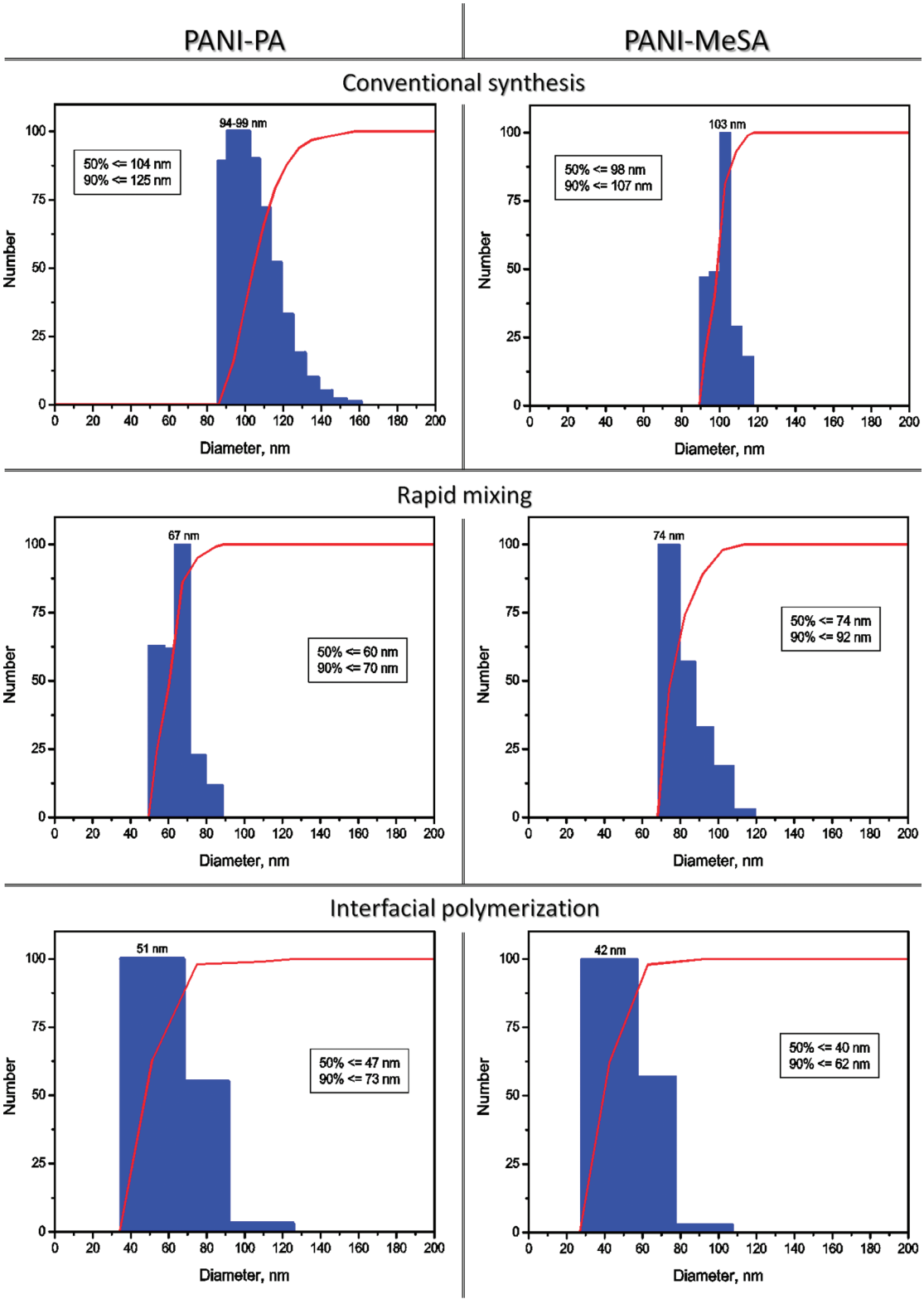

Figure 3. DLS results; relative number versus hydrodynamic diameters of PANI-PA particles (left column) and PANI-MeSA particles (right column) synthesized by the mentioned methods, and dispersed in acetone. Insets show the size for 50% and 90% of the distribution and red lines illustrate the cumulative number percentage of particles.

solvent. Aggregation of nanosized particles to a structure resembling a bunch of cauliflowers is seen for PANI dried from acetone (Figure 4a). These structures appear to be formed by particles in the size range detected by DLS (Figure 3) as shown by high resolution SEM (inset in Figure 4a). In contrast, the PANI powders formed by drying from NMP (Figure 4c) and chloroform

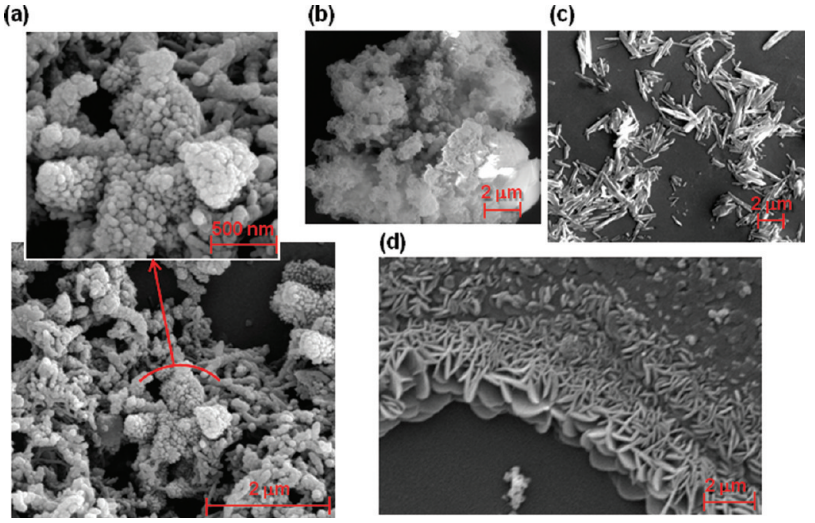

Figure 4. SEM micrographs showing the morphology of PANI-PA, synthesized by the rapid mixing method and dried from dispersions in (a) acetone, (b) water, (c) NMP, and (d) chloroform.

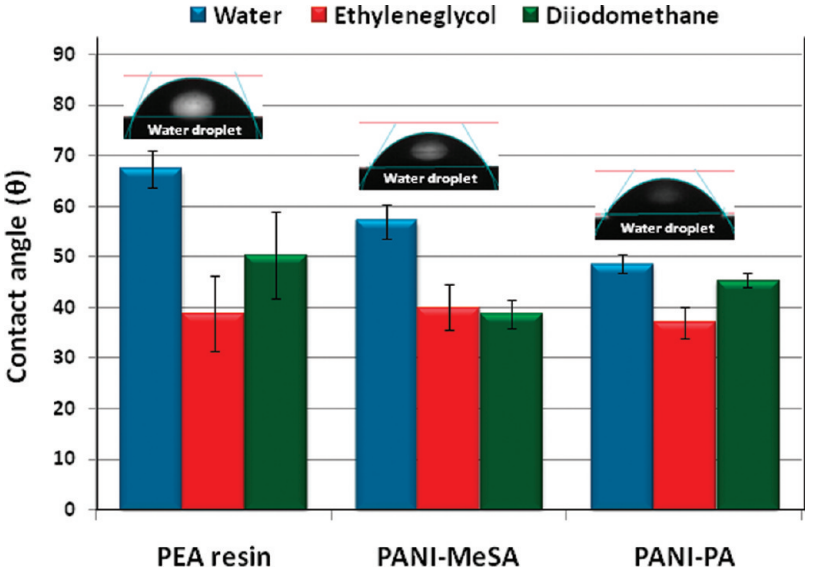

Figure 5. Contact angles of water, ethylene glycol, and diiodomethane droplets on cured PEA resin film, PANI-MeSA and PANI-PA pellets. Insets are photographs of water droplets on the corresponding surfaces.

(Figure 4d) show mostly fibrillar morphology, with the fibers being more separated in case of NMP. In NMP, the interactions with the dopant acid result in dedoped PANI (i.e., emeraldine base state),[43] and it has been suggested that hydrogen bonds between the carbonyl groups in NMP and the amine sites of emeraldine base PANI (i.e., C═O···H—N) counteracts large aggregation of the emeraldine base.[44] Because acetone has a dielectric constant in between that of NMP and chloroform, there is not a simple relation between the morphology of the dried particles and the dielectric constant of the solvent from which they are dried. Dispersions dried from water result mostly in large aggregates and clusters of particles (Figure 4b) that appear to be sintered together in contrast to the more open structure of the aggregates formed by drying from acetone. The PANI particles shape and morphology found here is quite different from the fibrillar structure reported by Huang et al.,[5] which emphasizes the intricate effects of synthesis medium and reactant concentrations. Wessling et al.[3] found that the PANI primary particles are of spherical nature with a diameter of about 10 nm, but frequently tend to aggregate to spherical secondary particles of up to 100 nm in size. They suggested that the secondary particles can also have fibrillar shape due to strong dipolar interactions that favor linear growth.

The results presented above suggest that PANI powder dried from acetone will be more readily redispersed than PANI dried from any of the other solvents tested. This rationalized why PANI powders, to be dispersed into liquid PEA resin, were dried from PANI/acetone solutions under ultrasonication.

3.2. Interfacial Energies. The average contact angle values determined for water, ethylene glycol, and diiodomethane on PANI pellets and PEA resin films are shown in Figure 5. The water contact angle of emeraldine salt PANI was found to be

below 50° for PANI-PA and below 60° for PANI-MeSA, which is consistent with values reported in the literature. For instance, Blinova et al.[26] determined the water contact angle as a function of doping medium acidity and found a decrease in contact angle (from 78° for PANI base down to 44° for PANI salt) by lowering the pH, i.e. by increasing the protonation level. We find slightly higher hydrophilicity of PANI doped with phosphoric acid comparing to PANI doped with methane sulfonic acid, and such dopant effects have been noted previously.[9,26]

The surface energy components of the tested materials were calculated according to eq 1, and the results are shown in Table 4. We note that the tested PANI samples are in conducting (emeraldine salt) form and the high γ^- value obtained is due to the amine groups present in the emeraldine salt chain that act as electron donors,[42] although imine groups (electron acceptors in emeraldine base) have been protonated by the doping process, as seen in Figure 1. The liquid PEA resin surface energy determined by the Pendant drop method was 46.2 mJ m^{-2}, which is somewhat higher than that of the cured resin, reflecting the fact that nonpolar groups in solid polymeric materials accumulate at interfaces toward air.[45,46] Such molecular reorientations introduce an uncertainty in the estimation of the interfacial energy between PANI and liquid PEA resin. In the following we utilized the resin surface energy components given in Table 3 to estimate the interfacial energy (γ_{12}) between resin and PANI, as calculated according to van Oss.[29]

$$\gamma_{12} = \gamma_{12}^{LW} + \gamma_{12}^{AB} = (\sqrt{\gamma_1^{LW}} - \sqrt{\gamma_2^{LW}})^2 + 2(\sqrt{\gamma_1^+\gamma_1^-} + \sqrt{\gamma_2^+\gamma_2^-} - \sqrt{\gamma_1^+\gamma_2^-} - \sqrt{\gamma_1^-\gamma_2^+}) \quad (4)$$

Table 4. Surface Energy Components (mJ m^{-2}) Calculated for the Tested Materials

	γ	γ^{LW}	γ^+	γ^-
cured PEA resin	40.7	34.0	0.8	13.7
PANI-PA	40.4	36.8	0.09	36.9
PANI-MeSA	41.9	40.2	0.03	27.0

It is clear from eq 4 that a pronounced polar cohesion of component 1 or 2 gives rise to higher γ_{12} value, whereas a strong polar adhesive interaction between the two components results in a decreased γ_{12}.[30]

The interfacial energy between PEA resin and PANI, $\gamma_{PEA/PANI}$, was found to be −1.9 mJ m^{-2} for PANI-MeSA and −2.8 mJ m^{-2} for PANI-PA. The negative values of the interfacial energy indicate that the free energy of interaction ($\Delta G_{121} = -2\gamma_{12}$) between two PANI particles immersed in the PEA resin is positive. This arises from the strong Lewis base character of PANI and the presence of some Lewis acid character for the PEA resin. We note that $\Delta G > 0$ indicates repulsion between PANI particles, signifying good dispersibility in the PEA resin.

The wetability behavior of liquid resin on PANI pellets was also investigated and the snapshots seen in Figure 6 illustrate the general behavior until full-wetting of the surface. The high viscosity of the PEA resin strongly influences the spreading behavior.

The base diameter of the drop expands during the first minute in contact with the surface. At the end of this stage the contact

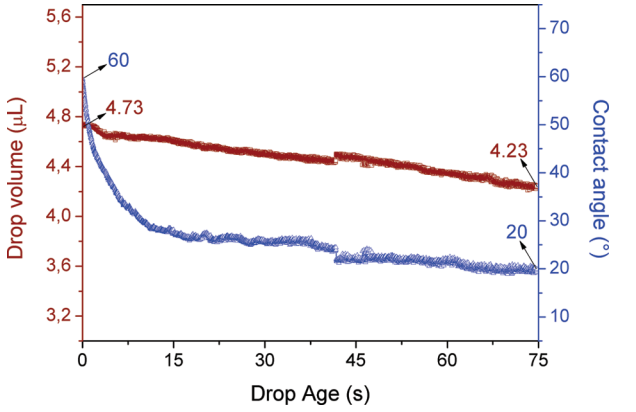

Figure 7. Changes in contact angle of PEA resin on PANI-PA pellet (right *Y*-axis and blue open triangle symbol) and drop volume (left *Y*-axis and red open square symbol) by time.

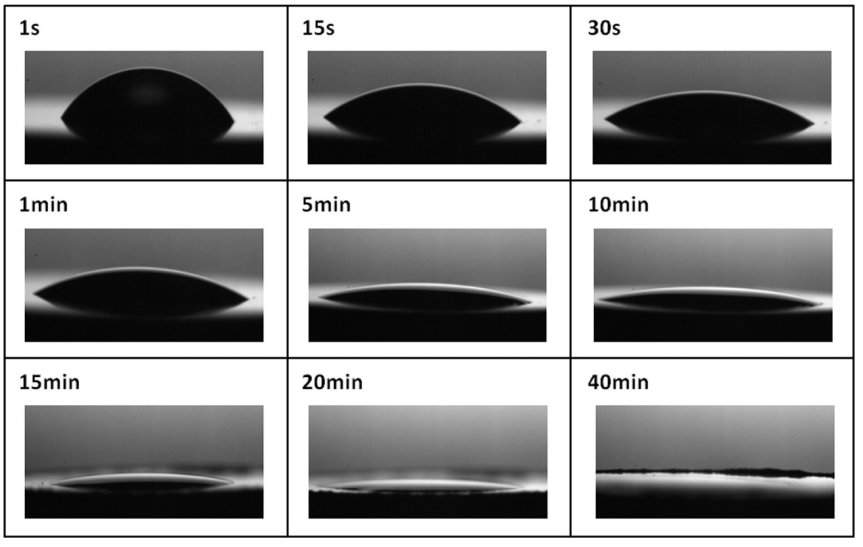

Figure 6. Liquid PEA resin drop shape on a PANI-PA pellet surface as a function of time. Images captured by a high-resolution CCD camera while the drop is illuminated from the other side. $\theta \rightarrow 0$, and the prolonged full-spreading relaxation time is due to the high viscosity of the PEA resin.

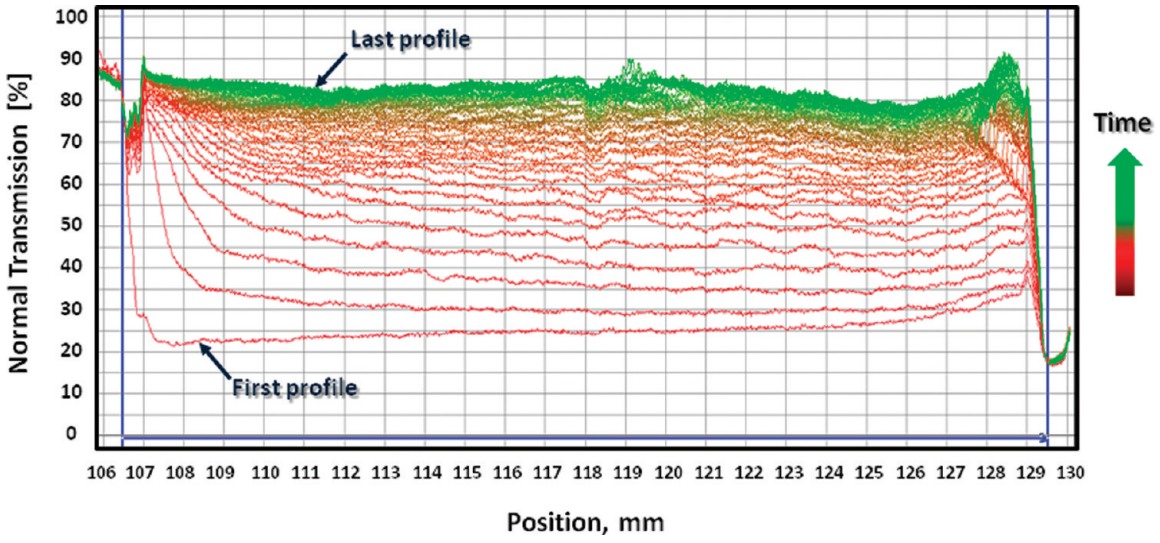

Figure 8. Transmission profiles of a 0.05 wt.% PANI-PA dispersion in liquid PEA resin, collected at 4000 rpm and 25 °C by a LUMiSizer dispersion analyzer. Color scale from red to green shows the time progress of the profiles (every 5 profile of the recorded profiles with Δt = 300 s are shown here). The bottom of the test tube is at a position of 130 mm.

line becomes pinned and the contact angle is about 20°. A further reduction in contact angle occurs as the PEA resin imbibes into the micropores of the PANI pellet. By further imbibition, the base diameter of the droplet starts contracting (compare the image after 10 min and after 15 min), and this occurs when the contact angle is reduced to a few degrees. Finally, a part of the PEA resin droplet that is not taken up by PANI forms a thin layer on the pellet surface. From this sequence of events we can conclude that the advancing contact angle is about 20−25° and the receding angle is close to zero, again indicating good compatibility between liquid PEA resin and PANI.

The initial stage of the wetting of PEA on PANI is illustrated in Figure 7, which provides quantitative data on the changes in the contact angle and PEA drop volume by time. The initial spreading, most pronounced during the first 15 s, results in a quick lowering of the contact angle, whereas the droplet volume decreases smoothly with time due to imbibition. It should be noted that PEA is a solvent-free resin and the change in droplet volume is thus not due to evaporation.

3.3. Dispersion Stability and Particle Size Distribution in Resin. PANI-PA synthesized by the rapid mixing method was chosen for the composite preparation, due to good dispersibility in acetone, concluded from DLS results, and good compatibility with PEA resin, concluded from interfacial tension studies. Furthermore, the phosphoric acid dopant may have an additional benefit in some applications as adhesion to metals is promoted by the presence of phosphates,[47] and specially that there already exists phosphorus-containing adhesion promoters in the resin base formulation.

Centrifugal Sedimentation. An example of the centrifugation transmission profiles versus position and time is shown in Figure 8.

The demixing process is followed by the changes in transmission profiles versus time. The high transmission at the end of the experiment (about 85% in Figure 8) indicates full-sedimentation. The slowly declining transmission profiles versus position reflect the particle size distribution, with particles settling by different velocities depending on their size.

Dispersion Stability. The clarification of the PANI-PA dispersion in PEA during sedimentation is illustrated in Figure 9 in terms of the integrated transmission profile in the middle region of the test tube versus the centrifugation time. These changes are directly related to the dispersion stability and the sedimentation rate. The initial change in transmission is fairly low for all samples, indicating slow sedimentation, which corresponds to high stability of the dispersions.[33] This is primarily an effect of the high viscosity of the liquid, but also consistent with the repulsive particle−particle interactions. It should be noted that the very slow change in transmission in the first hours for the samples with high PANI-PA content is likely due to the difficulty in tracking changes in transmission through concentrated and highly absorbing solutions. Therefore the curves are shifted toward larger times with increasing PANI concentration. Another reason could be that hindered settling becomes important in the more concentrated systems, where repulsion between the dispersed particles counteract formation of a compact sediment. The shape of the integral transmission curve for the highest PANI content (4 wt.%) appears distinctly different from those at the lower concentrations, suggesting that hindered settling is of importance in this case.

Particle Size Distribution in Resin. The particle size (equivalent Stokes diameter) was calculated from the transmission data using eqs 2 and 3. The particle size distribution obtained from the transmission profiles for the 1.5 wt.% PANI-PA/PEA dispersion is illustrated in Figure 10. Statistical analysis shows that 50% of the particles have a size below 200 nm and 90% of the distribution is less than 400 nm. Note that this range of particle size is achieved for PANI powders prepared by ultrasonically drying from acetone solution and in a solvent-free and high viscous resin.

The small-size distribution peak (at around 100 nm) is close to that found for PANI dispersed in acetone (Figure 3). The overall larger particle size distribution as compared to the DLS results is due to the addition of PANI to PEA resin as dry powder, and as seen in the SEM images (Figure 4) the drying process results in aggregate formation. This highlights the importance of determining the particle size directly in the resin matrix. The larger fraction seen in Figure 10 is due to aggregates that could not be dispersed under our mixing conditions. One should keep it in

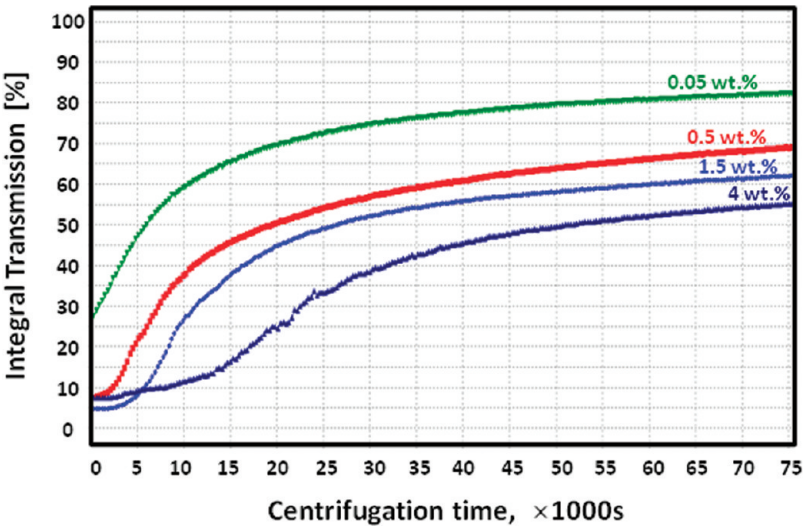

Figure 9. Integral transmission versus centrifugation time for PANI-PA/PEA dispersions with different PANI content noted on the curves (integration in the middle region; position 106.5−129.5 mm of the transmission profiles). The experiment was performed at 4000 rpm and 25 °C by a LUMiSizer dispersion analyzer.

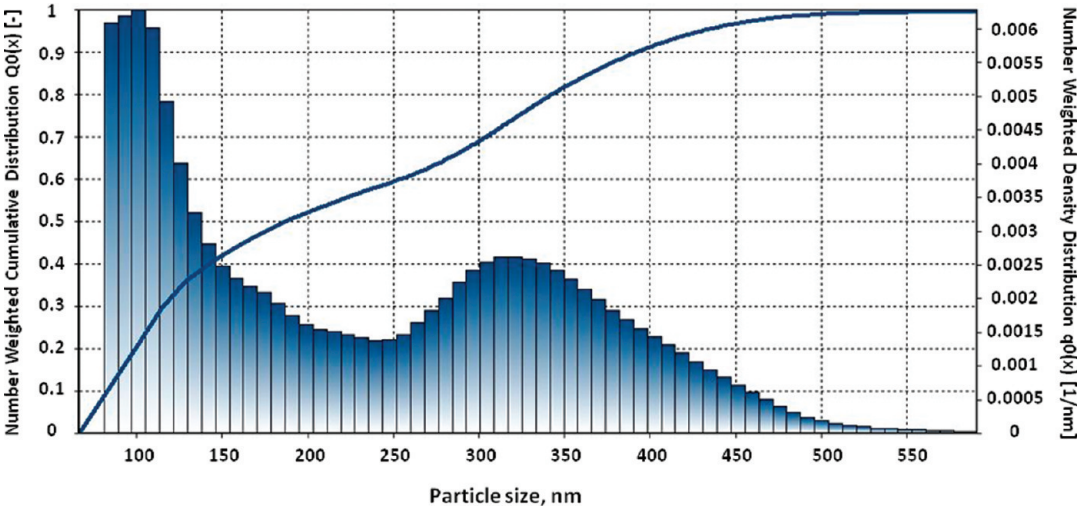

Figure 10. Number weighted particle size distribution of 1.5 wt.% PANI-PA, synthesized by the rapid mixing method, dispersed in liquid PEA resin. The size distribution was calculated from centrifugal sedimentation data collected at 4000 rpm and 25 °C by a LUMiSizer dispersion analyzer.

mind that the negative interfacial energies between PANI and PEA suggests that if the powders are added as individual particles, or the energy input needed to disperse the aggregates is provided by proper mixing, repulsive forces between particles in the resin will keep them separated.

4. CONCLUSIONS

The results reported in this work provide guidelines for preparation of homogeneous dispersions of PANI in an insulating polymer matrix. Doped polyaniline (PANI) with conductivities in the order of 10^{-2} to 10^{-1} Scm^{-1} were synthesized by the conventional, rapid mixing and interfacial polymerization methods. Of these methods, the rapid mixing was preferred since it provided a large quantity of PANI in the form of small particles. The doped PANI-PA particles prepared in this way dispersed well in acetone, and DLS measurements showed 90% of the particles to be less than 70 nm in diameter. The particles dried from acetone under sonication aggregated in loose cauliflower-like structures, as determined by SEM analysis, and they could largely be redispersed. Thus, this appears to be a suitable method for preparation of redispersible dry PANI powder.

The surface properties of PANI-PA and PANI-MeSA in emeraldine salt form were determined as the apolar, Lewis acid and Lewis base components of the surface energy. It was found that the Lewis base component of the PANIs was large, indicating that the interfacial energy toward liquids with some Lewis acid surface energy component should be small. Indeed, slightly negative interfacial energies between PANI and polyester acrylate (PEA) resin were found and suggested good compatibility of the two components.

Centrifugal sedimentation analysis of PANI-PA dispersions in PEA demonstrated a high stability. The particle size distribution

in PEA resin was shifted toward somewhat larger sizes as compared to that found in acetone, but nevertheless 90% of the particles were found to be below 400 nm. This is promising since small particle sizes favor high dispersion homogeneity and a low percolation threshold, and indicate that a low PANI content may be sufficient for achieving, e.g., good corrosion protection without compromising the material properties of the host polymer matrix.

AUTHOR INFORMATION

Corresponding Author

*Tel: +46-87906670. Fax: +46-8208284. E-mail: shadijz@kth.se.

ACKNOWLEDGMENT

The authors acknowledge valuable help from Magnus Bergström and Rubén Álvarez Asencio; Division of Surface and Corrosion Science, KTH, and from Asaf Oko; Institute for Surface Chemistry, YKI. Financial support from SSF; The Microstructure, Corrosion and Friction Program, and from SSAB EMEA are also gratefully acknowledged. Marc Heylen from Cytec Surface Specialties, Belgium, is acknowledged for providing the UV curing resin.

REFERENCES

(1) Eftekhari, A. *Nanostructured Conductive Polymers*, 1st ed.; John Wiley & Sons Ltd.: Chichester, U.K., 2010.
(2) Bhadra, S.; Khastgir, D.; Singha, N. K.; Lee, J. H. *Prog. Polym. Sci.* **2009**, *34*, 783–810.
(3) Wessling, B. In *Handbook of Conducting Polymers*; Terje, A., Skotheim, R. L. E., Reynolds, J. R., Ed.; Marcel Dekker.: New York, 1998.
(4) Huang, J.; Kaner, R. B. *Angew. Chem., Int. Ed.* **2004**, *43*, 5817–5821.
(5) Huang, J. *Pure Appl. Chem.* **2006**, *78*, 15–27.
(6) Wu, X.; Qi, S.; He, J.; Duan, G. *J. Mater. Sci.* **2010**, *45*, 483–489.
(7) Mandal, B. M. *Bull. Mater. Sci.* **1998**, *21*, 161–165.
(8) Banerjee, P.; Mandal, B. M. *Macromolecules* **1995**, *28*, 3940–3943.
(9) Zhang, Z.; Wei, Z.; Wan, M. *Macromolecules* **2002**, *35*, 5937–5942.
(10) Stejskal, J.; Sulimenko, T.; Prokeš, J.; Sapurina, I. *Colloid Polym. Sci.* **2000**, *278*, 654–658.
(11) Gospodinova, N.; Mokreva, P.; Terlemezyan, L. *J. Chem. Soc., Chem. Commun.* **1992**, 923–924.
(12) Vincent, B.; Waterson *J. Chem. Soc., Chem. Commun.* **1990** 683–684.
(13) Ma, H.-y.; Li, Y.-w.; Yang, S.-x.; Cao, F.; Gong, J.; Deng, Y.-l. *J. Phys. Chem. C* **2010**, *114*, 9264–9269.
(14) Pan, L. J.; Pu, L.; Shi, Y.; Song, S. Y.; Xu, Z.; Zhang, R.; Zheng, Y. D. *Adv. Mater.* **2007**, *19*, 461–464.
(15) Chang, H.; Yuan, Y.; Shi, N.; Guan, Y. *Anal. Chem.* **2007**, *79*, 5111–5115.
(16) Liu, J.-M.; Yang, S. C. *J. Chem. Soc., Chem. Commun.* **1991** 1529–1531.
(17) Marinakos, S. M.; Shultz, D. A.; Feldheim, D. L. *Adv. Mater.* **1999**, *11*, 34–37.
(18) Wan, M.; Li, J. *J. Polym. Sci., Part A: Polym. Chem.* **2000**, *38* 2359–2364.
(19) Cao, Y.; Andreatta, A.; Heeger, A. J.; Smith, P. *Polymer* **1989**, *30*, 2305–2311.
(20) Wessling, B. *Synth. Met.* **1991**, *45*, 119–149.
(21) Pron, A.; Nicolau, Y.; Genoud, F.; Nechtschein, M. *J. Appl. Polym. Sci.* **1997**, *63*, 971–977.
(22) Angelopoulos, M.; Asturias, G. E.; Ermer, S. P.; Ray, A.; Scherr, E. M.; Macdiarmid, A. G.; Akhtar, M.; Kiss, Z.; Epstein, A. J. *Mol. Cryst. Liq. Cryst.* **1988**, *160*, 151–163.
(23) Andreatta, A.; Cao, Y.; Chiang, J. C.; Heeger, A. J.; Smith, P. *Synth. Met.* **1988**, *26*, 383–389.
(24) Yang, C. Y.; Cao, Y.; Smith, P.; Heeger, A. J. *Synth. Met.* **1993**, *53*, 293–301.
(25) Adhikari, A.; Claesson, P.; Pan, J.; Leygraf, C.; Dedinaite, A.; Blomberg, E. *Electrochim. Acta* **2008**, *53*, 4239–4247.
(26) Blinova, N. V.; Stejskal, J.; Trchová, M.; Prokeš, J. *Polym. Int.* **2008**, *57*, 66–69.
(27) Provencher, S. W. *Makromol. Chem.* **1979**, *180*, 201–209.
(28) Brown, W. *Light Scattering Principles and Development*; Oxford University Press: New York, 1996.
(29) Van Oss, C. J. *Colloids Surf., A* **1993**, *78*, 1–49.
(30) Van Oss, C. J.; Chaudhury, M. K.; Good, R. J. *Chem. Rev.* **1988**, *88*, 927–941.
(31) Hansen, F. K.; Rødsrud, G. *J. Colloid Interface Sci.* **1991**, *141*, 1–9.
(32) Stauffer, C. E. *J. Phys. Chem.* **1965**, *69*, 1933–1938.
(33) Lerche, D. *J. Dispersion Sci. Technol.* **2002**, *23*, 699–709.
(34) Krause, B.; Petzold, G.; Pegel, S.; Pötschke, P. *Carbon* **2009**, *47*, 602–612.
(35) Petzold, G.; Goltzsche, C.; Mende, M.; Schwarz, S.; Jaeger, W. *J. Appl. Polym. Sci.* **2009**, *114*, 696–704.
(36) Detloff, T.; Sobisch, T.; Lerche, D. *Part. Part. Syst. Charact.* **2006**, *23*, 184–187.
(37) Krause, B.; Mende, M.; Pötschke, P.; Petzold, G. *Carbon* **2010**, *48*, 2746–2754.
(38) Sathiyanarayanan, S.; Muthkrishnan, S.; Venkatachari, G. *Electrochim. Acta* **2006**, *51*, 6313–6319.
(39) Abdiryim, T.; Xiao-Gang, Z.; Jamal, R. *Mater. Chem. Phys.* **2005**, *90*, 367–372.
(40) Vera, A, R.; Romero, B, H.; Ahumada, E. *J. Chil. Chem. Soc.* **2003** *48*, 35–40.
(41) Pu, H.-t.; Qiao, L.; Liu, Q.-z.; Yang, Z.-l. *Eur. Polym. J.* **2005**, *41*, 2505–2510.
(42) Pron, A.; Rannou, P. *Prog. Polym. Sci.* **2002**, *27*, 135–190.
(43) Geng, Y.; Li, J.; Jing, X.; Wang, F. *Synth. Met.* **1997**, *84*, 97–98.
(44) Zheng, W.; Angelopoulos, M.; Epstein, A. J.; MacDiarmid, A. G. *Macromolecules* **1997**, *30*, 7634–7637.
(45) Wang, J. H.; Claesson, P. M.; Parker, J. L.; Yasuda, H. *Langmuir* **1994**, *10*, 3887–3897.
(46) Chen, Z.; Shen, Y. R.; Somorjai, G. A. *Annu. Rev. Phys. Chem.* **2002**, *53*, 437–465.
(47) Mequanint, K.; Sanderson, R.; Pasch, H. *J. Appl. Polym. Sci.* **2003**, *88*, 900–907.